Numerical simulation of acoustic waveguides for Webster-Lokshin model using diffusive representations

Thomas Hélie[1] and Denis Matignon[2*]

[1] IRCAM, Analysis-Synthesis team, 1, place Igor Stravinsky,
   F-75 004 Paris, France
[2] INRIA, Sosso project, domaine de Voluceau-Rocquencourt, B.P. 105,
   F-78153 Le Chesnay, France

1 Introduction

This paper deals with the numerical simulation of acoustic wave propagation in axisymmetric waveguides with varying cross-section using a Webster-Lokshin model. Splitting the pipe into pieces on which the model coefficients are nearly constant, analytical solutions are derived in the Laplace domain, enabling for the realization of the propagation by concatenating scattering matrices of transfer functions (§ 2). These functions involve standard differential and delay operators, as well as pseudo-differential operators of diffusive type, induced by both the viscothermal losses and the curvature. These operators are explicitly decomposed thanks to an asymptotic expansion, and the diffusive ones may be defined and classified (§ 3). Various equivalent diffusive realizations may be proposed, that are deeply linked to choices of cuts in the complex analysis of the transfer functions. Then, finite order approximations are given for their simulation (§ 4).

2 Deriving the model

2.1 Acoustic model

A mono-dimensional model of the propagation of the acoustic pressure p in axisymmetric waveguides including viscothermal losses on the wall has been derived in [1, chap 1], assuming the quasi-sphericity of isobars near the wall. Defining in the Laplace domain $\widehat{\psi}(z,s) = R(z)\,\widehat{p}(z,s)$ where s is the Laplace variable, z is the curvilinear ordinate measuring the arc length of the wall, and $R(z)$ is the radius of the guide, the Webster-Lokshin model may be written:

$$\partial_z^2 \widehat{\psi}_z(s) - \left[\left(\frac{s}{c}\right)^2 + 2\,\varepsilon(z)\left(\frac{s}{c}\right)^{\frac{3}{2}} + \Upsilon(z) \right] \widehat{\psi}_z(s) = 0. \tag{1}$$

c is the sound speed, $\Upsilon(z) = R''(z)/R(z)$ the curvature, and $\varepsilon(z) = \lambda \frac{\sqrt{1-R'(z)^2}}{R(z)}$ quantifies the effect of the viscothermal losses. Note that contant curvatures

* on sabbatical leave from ENST, TSI dept. & CNRS, URA 820. 46, rue Barrault
   F-75634 Paris Cedex 13, FRANCE.

correspond to cylinders or cones ($\Upsilon = 0$), exponential or catenoidal shapes ($\Upsilon > 0$), and sinusoidal shapes ($\Upsilon < 0$), for the curvilinear ordinate z. For short pieces of guide on which Υ and ε may be approximated by their constant mean value, Eq. (1) has the analytic solution $\widehat{\psi}_z(s) = A(s)\mathrm{e}^{z\,\Gamma(s)} + B(s)\mathrm{e}^{-z\,\Gamma(s)}$ where $\Gamma(s)$ is a square root of $\left(\frac{s}{c}\right)^2 + 2\varepsilon\left(\frac{s}{c}\right)^{\frac{3}{2}} + \Upsilon$.

2.2   Scattering matrix

The waves $\widehat{p}^{\pm}(z,s) = (\widehat{p}(z,s) \mp \rho\,c\,\partial_z\widehat{p})/2$ defined in [2] are locally outwardly ($\widehat{p}^+$) and inwardly ($\widehat{p}^-$) directed. For a $\mathcal{C}^1$-regular profile $R(z)$, their connection at z^* is simply given by $\widehat{p}^{\pm}_n(z^*,s) = \widehat{p}^{\pm}_{n+1}(z^*,s)$ where n and $n+1$ index two concatenated pieces of guide. For this last reason, we are interested in the time-domain simulation of the scattering matrix defined for $\widehat{\psi}^{\pm}_z = R(z)\,\widehat{p}(z,s)$.

For convenience, we consider the adimensional problem ($c = |\Upsilon| = 1$, and $z \in [0,1]$, $\beta \propto \varepsilon$, and $\Gamma(s)$ is a square root of $s^2 + 2\beta s^{\frac{3}{2}} + \mathrm{sign}(\Upsilon)$). This yields

$$
\begin{bmatrix} \widehat{\psi}^+_L(s) \\ \widehat{\psi}^-_0(s) \end{bmatrix} = \begin{bmatrix} \mathcal{T}(s) & \mathcal{R}_1(s) \\ \mathcal{R}_0(s) & \mathcal{T}(s) \end{bmatrix} \begin{bmatrix} \widehat{\psi}^+_0(s) \\ \widehat{\psi}^-_1(s) \end{bmatrix}. \tag{2}
$$

where the transmission $\mathcal{T}$ and the reflexion $\mathcal{R}_z$ at the input ($z=0$) or the output ($z=1$) are rational functions with respect to s, $\Gamma(s)$, and $\mathrm{e}^{-\tau\Gamma(s)}$. In § 3, we investigate $\mathrm{e}^{-\tau\Gamma(s)}$ for the case $\Upsilon \geq 0$ which is reduced to the standard delay operator $\mathrm{e}^{-\tau s}$ for ideal pipes ($\Upsilon = \epsilon = 0$) [1, chap. 3].

3   Using diffusive representations

The impulse response of a pseudo-differential operator of diffusive type can be decomposed on a continuous family of purely damped exponentials with weight μ. A diffusive realization helps transforming a non-local in time pseudo-differential equation into a first-order differential equation on a Hilbert state-space, which allows for stability analysis; this approach reveals useful for both theoretical and numerical treatment of pseudo-differential equations. We refer to [7, § 5.] for the treatment of completely monotone kernels, [6] for diffusive representations of pseudo-differential operators, and [5] for links between fractional differential operators and diffusive representations.

For the simulation of $\mathrm{e}^{-\tau\Gamma(s)}$, we proceed as explained in § 3.4 : it is a generalization of diffusive representations of the first and second kind, as recalled in § 3.2 and § 3.3; it is based on an asymptotic expansion presented in § 3.1.

3.1   Decomposition of the transfer function

The asymptotic expansion of $\Gamma(s)$ for $|s| \to +\infty$ reads $\Gamma(s) = s + \beta\sqrt{s} - \frac{\beta^2}{2} + o(1)$. Thus, $\mathrm{e}^{-\tau\,\Gamma(s)}$ may be decomposed into several transfer functions, namely: $\mathrm{e}^{-\tau\Gamma(s)} = \mathrm{e}^{-\tau s}\,\mathrm{e}^{-\tau\beta\sqrt{s}}\,\mathcal{H}(s)$, where $\mathrm{e}^{-\tau s}$ is a pure delay, $\mathrm{e}^{-\tau\beta\sqrt{s}}$ is diffusive of the first kind (see § 3.2), and $\mathrm{e}^{-\tau(\Gamma(s)-s-\beta\sqrt{s}+\beta^2/2)}$ is diffusive in a generalized sense (see § 3.4). The last two operators are investigated below.

3.2   Diffusive representation of the first kind

The transfer function $\mathcal{H}_1(s) = \mathrm{e}^{-\sqrt{s}}$, understood with a cut on $\mathbb{R}^-$, is known to be diffusive of the first kind, with an extension defined in [6, § 5.2], with density $\mu_1(\xi) = \frac{\sin(\sqrt{\xi})}{\pi\,\xi}$ for $\xi > 0$. It fulfills the well-posedness condition $\int_0^{+\infty} \frac{|\mu_1(\xi)|}{1+\xi}\, d\xi < \infty$. Thus, $\mathcal{H}_1(s) = s \int_0^{+\infty} \frac{\mu_1(\xi)}{s+\xi}\, d\xi$ gives rise to a natural realization of the transfer, as a superposition of basic first-order differential systems.

3.3   Diffusive representation of the second kind

A diffusive representation of the second kind may be directly used in the case $\beta = 0$. Then, $\mathrm{e}^{-\tau\,\Gamma(s)} = \mathrm{e}^{-\tau\sqrt{s^2+1}}$, where $\sqrt{s^2+1}$ may be defined by $\sqrt{s-i}\,\sqrt{s+i}$, $\sqrt{z}$ being still understood with a cut for $z \in \mathbb{R}^-$. The two branchpoints $+i$ and $-i$ are thus associated to the cuts $i + \mathbb{R}^-$ and $-i + \mathbb{R}^-$, respectively. A diffusive representation of such an operator may be derived from complex-valued densities computed on these two cuts, as described in [5, § 3.3] for $(s^2 + 1)^{-1/2}$.
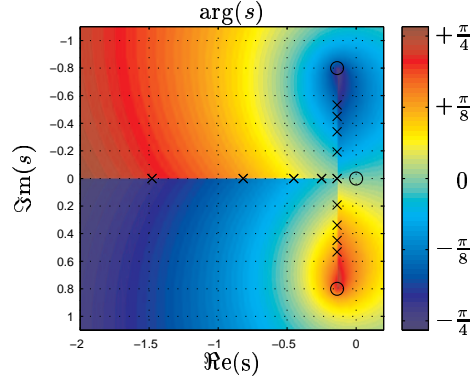

Figure1: Phase of $\mathcal{H}_2(s)$ defined for the cut $[s_1, s_2] \cup \mathbb{R}^-$, $\tau = 1$, and $\beta = 0.3$. Branchpoints are represented by $\circ$ and the poles of the approximating transfer function by $\times$.

3.4   Generalized diffusive representation

When $\beta \neq 0$, some more care must be taken for $\mathcal{H}_2(s) = \mathrm{e}^{-\tau(\Gamma(s)-s)}$, and the previous ideas must be adapted.

Analysis. $\forall \beta > 0$, $\Gamma(s)$ has two zeros s_1 and $s_2 = \overline{s_1}$ with $\Re\mathrm{e}(s_{1,2}) < 0$ and $\Im\mathrm{m}(s_1) > 0$, thus leading to 4 branchpoints for $\mathcal{H}_2$, namely $0, s_1, s_2$ and a point at infinity, such as $-\infty$. This implies that $\Gamma(s)$ may be defined for any cuts made of $\mathbb{R}^-$ and a curve linking s_1 and s_2.

Diffusive representation of $e^{-\tau(\Gamma(s)-s)}$. Among the different compatible cuts, we can investigate either 3 parallel cuts (concatenation of § 3.2 and § 3.3), or a cross made of $\mathbb{R}^-$ and the vertical segment joining s_1 and s_2 (see Fig. 1). The corresponding density μ can be found analytically by limit formulas on either of these two cuts, after some quite tedious computations: in this case, μ directly accounts for the discontinuity of $\mathcal{H}_2(s)$ across the cut.

An alternative to diffusive representation of the second kind pioneered by [7, § 6.] and developped by [3] is the so-called Γ-contour. A regular curve $\Gamma \subset \mathbb{C}^-$ encircles all the singularities (poles, branchpoints, cuts, ...) of $\mathcal{H}_2(s)$; thus, by the inverse Laplace transform, we get a representation with a complex-valued density μ_Γ, expressed directly and continuously from $\mathcal{H}_2(s)$, for $s \in \Gamma$.

Realization with a Γ-contour. Although no differences in principle remain between realizations for Γ-contours and for cuts (a cut can even be seen as a limiting process of Γ-contour), this is not the case for realizations approximated by first-order linear constant-coefficient systems. Moreover, Γ-contours yield a density μ_Γ containing all the information carried by the encircled discontinuity, but under a somewhat averaged form. On the contrary, cuts yield a more focused information, since the density μ exactly measures the discontinuity.

The placement of the poles gives rise to an unlimited choice, and the question of finding a suitable if not minimal description is an interesting open question, as already noticed in [7, § 6.]. A trade-off must then be found between averaged information with a density computed continuously from the transfer function, and localized and accurate information with a density computed as a discontinuity of the same transfer function.

4   Numerical simulations with optimization

We now derive approximations of transfer functions by first-order linear constant-coefficient systems, stemming from the generalized diffusive realizations presented in § 3.4. The approximated model has the form $\widehat{\mathcal{M}}_\gamma(s)\,.\,\nu = \sum_{1 \leq k \leq K} \frac{\nu_k}{s - \gamma_k}$, where the set of poles $\gamma = \{\gamma_k\} \subset \Gamma$ is chosen with a hermitian symmetry. The set Γ may represent either a cut or a Γ-contour associated with the diffusive operator under consideration. The problem now consits of estimating $\nu = \{\nu_k\}$.

A first method computes ν_k analytically: Γ is described in the complex plane by $\xi \mapsto \gamma(\xi)$, and $\nu_k = \int_0^{+\infty} \mu(\gamma(\xi)) \Lambda_k(\xi)\, \gamma'(\xi)\, d\xi$, where Λ_k are interpolating functions (see e.g. [4] and [3]).

The second method, that is being used here for the *cross-cut*, consists of a least-square regularized optimization of $\{\nu_k\}$, minimizing the distance between $\mathcal{H}_2(i\omega)$ and $\widehat{\mathcal{M}}_\gamma(i\omega)\,.\,\nu$ for $\omega \in [\omega_{min}, \omega_{\max}]$. We take the following criterion:

$$\mathcal{C}_\epsilon(\nu) = \|\widehat{\mathcal{M}}_\gamma\,.\,\nu - \mathcal{H}_2\|^2_{L^2(\omega_{min},\omega_{\max})} + \epsilon_1 \sum_{\{k/\gamma_k \in [s_1,s_2]\}} |\nu_k|^2 + \epsilon_2 \sum_{\{k/\gamma_k \in \mathbb{R}^-\}} |\nu_k|^2 \quad (3)$$

where ϵ_1 and ϵ_2 are regularizing parameters for the oscillating and diffusive parts, respectively. An example of result obtained for this criterion and for the pole placement represented in Fig. 1 is given in Fig. 2. Note that the optimization may be adapted for H^p-norms, taking the measure $(1 + \omega^2)^{p/2} d\omega$.
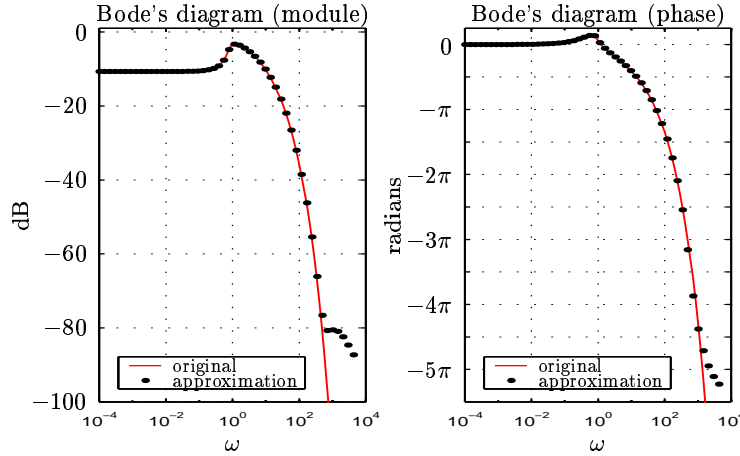
Figure2: Bode diagrams of the exact transfer function $\mathcal{H}_2(i\omega)$ and of $\left(\widehat{\mathcal{M}}_\gamma(i\omega).\nu\right)$ for $\tau = 1$, $\beta = 0.3$, $\epsilon_1 = 0$, $\epsilon_2 = 10^{-10}$, with 4 complex conjugate pairs of poles on $[s_1, s_2]$ and 16 poles on $\mathbb{R}^-$ ($\gamma_{min} = -10^3$). Poles are spaced with a geometric sequence.

5   Conclusion

Our method sums up as follows. We derive the transfer functions in the Laplace domain. We perform a complex analysis: asymptotic expansions, poles and branch-points, choice of cuts in the left-half complex plane. Finally, the parameters of the approximated model are optimized in a least-square sense on a path in the Laplace domain, using either the cuts or a Γ-contour encircling all the singularities; the error is evaluated in the frequency domain. The time-domain simulations can be done straightforwardly.

References

1. Th. Hélie *Modélisation physique d'instruments de musique en systèmes dynamiques et inversion*. PhD thesis, Université de Paris XI Orsay, December 2002.
2. E. Ducasse. *Modélisation et simulation dans le domaine temporel d'instruments à vent à anche simple en situation de jeu : méthodes et modèles*. PhD thesis, ENSAM, Bordeaux I, 2001.
3. M. Dunau. Représentations diffusives de seconde espèce : introduction et expérimentation. DEA d'Automatique, Toulouse, 2000.
4. D. Heleschewitz. *Analyse et simulation de systèmes différentiels fractionnaires et pseudo-différentiels linéaires sous représentation diffusive*. PhD thesis, ENST, December 2000.
5. D. Matignon. Stability properties for generalized fractional differential systems. *ESAIM: Proceedings*, 5:145–158, December 1998. *(Available on web)*
6. G. Montseny. Diffusive representation of pseudo-differential time-operators. *ESAIM: Proceedings*, 5:159–175, December 1998. *(Available on web)*
7. O. J. Staffans. Well-posedness and stabilizability of a viscoelastic equation in energy space. *Trans. Amer. Math. Soc.*, 345(2):527–575, October 1994.